Super-Heisenberg scaling in Hamiltonian parameter estimation in the long-range Kitaev chain

Jing Yang,[1,2,*] Shengshi Pang,[3,†] Adolfo del Campo,[1,4,‡] and Andrew N. Jordan[5,2,§]

[1] *Department of Physics and Materials Science, University of Luxembourg, L-1511 Luxembourg, Luxembourg*
[2] *Department of Physics and Astronomy, University of Rochester, Rochester, New York 14627, USA*
[3] *School of Physics, Sun Yat-Sen University, Guangzhou, Guangdong 510275, China*
[4] *Donostia International Physics Center, E-20018 San Sebastián, Spain*
[5] *Institute for Quantum Studies, Chapman University, 1 University Drive, Orange, California 92866, USA*

(Received 15 April 2021; accepted 21 January 2022; published 18 February 2022)

In quantum metrology, nonlinear many-body interactions can enhance the precision of Hamiltonian parameter estimation to surpass the Heisenberg scaling. Here, we consider the the estimation of the interaction strength in linear systems with long-range interactions and using the Kitaev chains as a case study, we establish a transition from the Heisenberg to super-Heisenberg scaling in the quantum Fisher information by varying the interaction range. We further show that quantum control can improve the prefactor of the quantum Fisher information. Our results explore the advantage of optimal quantum control and long-range interactions in many-body quantum metrology.

DOI: 10.1103/PhysRevResearch.4.013133

I. INTRODUCTION

Quantum metrology is a paradigmatic example of an emergent technology in which quantum resources can provide an advantage over its classical counterpart [1–4]. The general scheme for estimating the parameters in a Hamiltonian system is depicted in Fig. 1. Quantum mechanics provides two key ingredients improving the precision: (a) the coherence in state ρ_θ of the probe, which is controlled by the probe time T, and (b) entanglement, when N probes are allowed in a single round, which can be introduced in the initial state or generated via many-body interactions during the sensing process. According to the quantum Cramer-Rao bound, the uncertainty $\delta\hat{\theta}$ in the estimation of the parameter θ in Fig. 1 is governed by the quantum Fisher information $I(\theta)$ (QFI) as $\delta\hat{\theta} \geqslant 1/\sqrt{\nu I(\theta)}$, where ν is the number of repetitions of the process. The QFI plays a fundamental role in the geometry of the space of quantum states and has manifold applications, which include witnessing a quantum phase transition [5–8], critical sensing [9–12], and detecting multipartite entanglement [13–15].

Recently, optimal control has been shown to offer a new arena for enhancing quantum parameter estimation [16–18]. The interplay between quantum control theory and quantum many-body systems is yet to be undertaken, and it is crucial to understand quantum parameter estimation of coupling constants in realistic systems with long-range interactions. In the Hamiltonian parameter estimation of noninteracting spin systems, the maximum possible QFI scales linearly with the number of probes for an uncorrelated initial state, known as the shot-noise limit [19]. The scaling becomes quadratic if the probes are initially prepared in the Greenberger-Horne-Zeilinge (GHZ) state with maximum entanglement, known as the Heisenberg scaling (HS) [19]. This naturally motivates the idea of surpassing the HS, reaching the so-called super-HS scaling by introducing nonlinear interactions in the sensing Hamiltonian [20–22]. These works have led to the intuitive belief that surpassing the HS requires nonlinear interactions.

However, one should note that all the previous analyses of QFI in many-body quantum metrology is restricted to many-body spin systems. Therefore, it is not *a priori* true that the aforementioned belief would be still valid for fermions. In this paper, we emphasize this belief needs careful examinations in

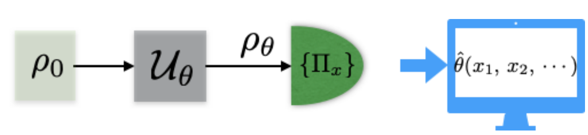

FIG. 1. A typical round in quantum metrology consisting of four steps (i) Preparing an initial quantum state ρ_0. (ii) Evolving the initial-state ρ_0 under a parameter θ-dependent unitary quantum channels $\mathcal{U}_\theta$ to obtain a parameter-dependent state ρ_θ. (iii) Performing a quantum measurement described by the positive operator-valued measure operators $\{\Pi_x\}$ on state ρ_θ to get data x_n. (iv) Steps (i)–(iii) can be run multiple times in parallel or a sequential scheme [19,21], which generates a large number of measurement data $\{x_1, x_2, \ldots\}$. Processing the data with the maximum likelihood estimator $\hat{\theta}(x_1, x_2, \ldots)$ saturates the classical-Cramér-Rao bound.

*jing.yang@uni.lu
†pangshsh@mail.sysu.edu.cn
‡adolfo.delcampo@uni.lu
§jordan@chapman.edu

the sense that linear fermionic systems can lead to different scaling of the QFI, comparing to the scaling for linear spin systems. In particular, the latter can lead to the super-HS scaling behavior with slowly decaying long-range interactions. We explore the Hamiltonian parameter estimation in linear systems with long-range interactions using a case study of the generalization of the long-range Kitaev (LRK) chain [23–25] to allow for general decay laws of the long-range interactions. By focusing on the estimation of the long-range superconducting strength, we establish that super-HS can be achieved in the case of slowly decaying *linear* long-range interactions. Indeed, we observe a transition from HS to super-HS for a specific value of the exponent governing the decay law of the interactions. In all cases, quantum control may improve the prefactor of the scaling of the QFI as a function of the the number of lattice sites.

II. HAMILTONIAN ESTIMATION OF THE LRK MODEL

We consider parameter estimation with a general time-dependent Hamiltonian $H_\theta(t)$, where θ is the estimation parameter and the parametric dependence is general, i.e., not necessarily multiplicative. The effective generator for the parameter estimation is defined as $|\psi_\theta\rangle = e^{-iG_\theta}|\psi_0\rangle$ [21], where $|\psi_0\rangle$ is the initial state and $|\psi_\theta\rangle$ is the effective parameter-dependent state which gives the same QFI as the true physical state [26]. For a general Hamiltonian it is given by [17,21,27]

$$G_\theta = \int_0^T \mathcal{U}_\theta^\dagger(\tau)\partial_\theta H_\theta(\tau)\mathcal{U}_\theta(\tau)d\tau,$$

where $\mathcal{U}_\theta(\tau)$ is the evolution operator. Once the generator is obtained, the quantum Fisher information is given by $I(\theta) = 4\,\mathrm{Var}[G_\theta]|_{|\psi_0\rangle}$. Maximization over all the possible initial states gives

$$I(\theta) = [\vartheta_{\max}(T) - \vartheta_{\min}(T)]^2, \tag{1}$$

where $|\vartheta_{\min}(T)\rangle$ and $|\vartheta_{\max}(T)\rangle$ as the eigenvectors that corresponding to the minimum and maximum eigenvalues of G_θ and the corresponding initial state is prepared in an equal superposition between $|\vartheta_{\max}(T)\rangle$ and $|\vartheta_{\min}(T)\rangle$. When coherent optimal controls are possible, one can further optimize the QFI over the unitary dynamics appear in the generator G_θ. We denote the eigenstates of $\partial_\theta H_\theta(t)$ at the instant time t as $|\chi_n(t)\rangle$. It turns out the optimal unitary dynamics is the one which steers the state always towards $|\chi_n(t)\rangle$, if one starts with $|\chi_0(0)\rangle$ [17]. With this intuition, it is easily found that the total Hamiltonian after including the control is

$$H_{\mathrm{tot}}(t) = i\hbar\,\partial_t\mathcal{U}_{c\theta}(t)\mathcal{U}_{c\theta}^{-1}(t), \tag{2}$$

where

$$\mathcal{U}_{c\theta}(t) = \sum_n |\chi_n(t)\rangle\langle\chi_n(0)| \tag{3}$$

is a unitary operator formed by the eigenvectors of $\partial_\theta H_\theta(t)$. Therefore, the optimal control Hamiltonian is [28,29]

$$H_c(t) = H_{\mathrm{tot}}(t) - H_\theta(t). \tag{4}$$

When optimal control is applied, the generator is $G_\theta = \sum_n |\chi_n(0)\rangle\langle\chi_n(0)| \int_0^T \chi_n(\tau)d\tau$. Thus, the upper bound of the QFI after optimization over the initial states and unitary dynamics is

$$I_0(\theta) = \left(\int_0^T [\chi_{\max}(\tau) - \chi_{\min}(\tau)]d\tau\right)^2, \tag{5}$$

where $\chi_{\max}(t)$ and $\chi_{\min}(t)$ are the maximum and minimum eigenvalues of $\partial_\theta H_\theta(t)$. The optimal initial state is the equal superposition between $|\chi_{\min}(0)\rangle$ and $|\chi_{\min}(0)\rangle$. For time-independent Hamiltonians, $I_0(\theta)$ is simply proportional to the square of the difference of the maximum and minimum eigenvalues of $\partial_\theta H_\theta$, with the prefactor $4T^2$.

Now we consider H_θ be the LRK Hamiltonian [23],

$$H_\theta = -\frac{J}{2}\sum_{j=1}^N (a_j^\dagger a_{j+1} + a_{j+1}^\dagger a_j) - \mu\sum_{j=1}^N\left(a_j^\dagger a_j - \frac{1}{2}\right) + \frac{\Delta}{2}\sum_{j=1}^{N-1}\sum_{l=1}^{N-j}\kappa_{l,\alpha}(a_j a_{j+l} + a_{j+l}^\dagger a_j^\dagger), \tag{6}$$

where considering a unit lattice spacing, J represents the tunneling rate between nearest neighbors, μ is the chemical potential, Δ represents the strength of the superconducting p-wave pairing, N is the number of Fermionic lattice sites, and $\kappa_{l,\alpha}$ satisfies the symmetry property: $\kappa_{l,\alpha} = \kappa_{N-l,\alpha}$ for $1 \leqslant l \leqslant N/2$. Here, $\alpha \geqslant 0$ characterizes the decay property of the long-range interaction. Without loss of generality, we choose the normalization condition $\kappa_{1,\alpha} = 1$. The Kitaev chain has recently attracted broad attention as it supports noise-resilient Majorana zero modes at its two ends for open boundary conditions [30,31]. Recent works [23–25] have generalized the original model to the LRK chain, which contains long-range superconducting p-wave pairing, i.e., the last term on the right-hand side of Eq. (6). On the other hand, Eq. (6) may be implemented by a quantum simulator. Benchmarking such a quantum simulator would involve quantum parameter estimation of the parameters J, μ, and Δ, which naturally motivates subsequent analysis.

Note that by contrast to the power-law decay law in Ref. [23], we consider a general decay law $\kappa_{l,\alpha}$ which only requires the existence of a finite non-negative integer $Q \geqslant 0$ such that: (i) $\kappa_{x,\alpha}$ and its derivatives with respect to x up to $2Q$ order are bounded on $[1,\infty]$, and (ii) $\int_1^\infty \kappa_{x,\alpha}^{(2Q+1)}dx$ is finite where the superscript (q) denotes the qth derivative with respect to x. Specifically, we consider power-law interactions with $\kappa_{l,\alpha} = l^{-\alpha}$ as in the original proposal of the LRK model [23] and $\kappa_{l,\alpha} = (1+\ln l)^{-\alpha} (\alpha \geqslant 0)$ [32]. Assuming the antiperiodic boundary condition $a_j = -a_{j+N}$, the LRK Hamiltonian (6) can be diagonalized via the Bogoliubov transformation [15], yielding

$$H_\theta = \sum_k \epsilon_\theta(k)\eta_\theta^\dagger(k)\eta_\theta(k), \tag{7}$$

where $k = \frac{1}{2}\frac{2\pi}{N}, \frac{3}{2}\frac{2\pi}{N}\cdots\frac{2\pi}{N}(N-\frac{1}{2})$,

$$\epsilon_\theta(k) \equiv \sqrt{[\Delta f_\alpha(k)/2]^2 + (J\cos k + \mu)^2}, \tag{8}$$

and

$$f_\alpha(k) \equiv 2\sum_{l=1}^{N/2-1}\kappa_{l,\alpha}\sin(kl) + \kappa_{N/2,\alpha}. \tag{9}$$

The factor of 2 in front of $f_\alpha(k)$ accounts for the symmetry property of $\kappa_{l,\alpha}$. The generator G_θ can be diagonalized via the Bogoliubov transformation as (see Appendix A for details)

$$G_\theta = \sum_k \mathscr{E}_\theta(k)\psi_\theta^\dagger(k)\psi_\theta(k), \tag{10}$$

where the Fermionic operators $\psi_\theta^\dagger(k)$ and $\psi_\theta(k)$ are defined in Eq. (A20) and the spectrum is

$$\mathscr{E}_\theta(k) \equiv \big(T^2[\partial_\theta\epsilon_\theta(k)]^2 + \tfrac{1}{4}\xi_\theta^2(k)\sin^2[2\epsilon_\theta(k)T], \\ + \tfrac{1}{4}\xi_\theta^2(k)\{1-\cos[2\epsilon_\theta(k)T]\}^2\big)^{1/2}, \tag{11}$$

with

$$\xi_\theta(k) \equiv \partial_\theta \cos\phi_\theta(k)/\sin\phi_\theta(k), \tag{12}$$

$$\sin\phi_\theta(k) = -\Delta f_\alpha(k)/[2\epsilon_\theta(k)], \tag{13}$$

$$\cos\phi_\theta(k) = -(J\cos k + \mu)/\epsilon_\theta(k). \tag{14}$$

III. OPTIMAL CONTROL AND OPTIMAL INITIAL STATE

We next determine the optimal controls and optimal initial states for parameter estimation by using the spectral properties of $\partial_\theta H_\theta(t)$, for the different choices of the Hamiltonian parameter θ. According to Eq. (A1) in Appendix A, the representation of the LRK Hamiltonian in the momentum space, it is readily calculated that

$$\partial_J H = -\sum_k a^\dagger(k)a(k)\cos k, \tag{15}$$

$$\partial_\mu H = -\sum_k a^\dagger(k)a(k). \tag{16}$$

We note that $\partial_J H$ and $\partial_\mu H$ commute with each other. Thus, according to the preceding section, the optimal control for estimating J and μ is to cancel the long-range superconducting terms. The maximum and minimum eigenstates for $\partial_J H$ are

$$|\mathbb{1}/\mathbb{2}\rangle = \prod_{k,\cos k\leqslant 0} a^\dagger(k)\,|0\rangle\,, \tag{17}$$

and

$$|-\mathbb{1}/\mathbb{2}\rangle = \prod_{k,\cos k>0} a^\dagger(k)\,|0\rangle\,, \tag{18}$$

respectively. We adopt this notation since in momentum space both the maximum and the minimum eigenstates are half-occupied. The optimal initial state for estimating J under optimal control is

$$|\psi_0\rangle = \frac{1}{\sqrt{2}}(|\mathbb{1}/\mathbb{2}\rangle + |-\mathbb{1}/\mathbb{2}\rangle). \tag{19}$$

Similarly, for $\partial_\mu H$, the maximum eigenstate is $|0\rangle$, the vacuum state annihilated by $a(k)$ or a_j, and the minimum eigenstate is the fully occupied state in the momentum space, which we denote as

$$|\mathbb{1}\rangle = \prod_k a^\dagger(k)\,|0\rangle\,. \tag{20}$$

Therefore, the optimal initial state for estimating μ under optimal control is

$$|\psi_0\rangle = \frac{1}{\sqrt{2}}(|0\rangle + |\mathbb{1}\rangle). \tag{21}$$

The optimal control for the estimation of Δ is to cancel all the local interaction terms, including the tunneling and kinetic terms. We note that the diagonalization of $\partial_\Delta H$ is a special case for the diagonalization of the LRK Hamiltonian, corresponding to $J=\mu=0$ and $\Delta=1$. With this observation one finds

$$\partial_\Delta H = \frac{1}{2}\sum_k |f_\alpha(k)|b^\dagger(k)b(k),$$

where $b(k) = u_k a(k) + v_k a^\dagger(-k)$, $u_k = 1/2$, $v_k = -i/\sqrt{2}$ if $f_\alpha(k) \geqslant 0$ and $v_k = i/\sqrt{2}$ if $f_\alpha(k) < 0$. We note that $v_k = -v_{-k}$ because $f_\alpha(k)$ is an odd function of k. The minimum eigenstate of $\partial_\Delta H$ is the ground state annihilated by $b(k)$. According to the BCS ansatz, it is

$$|\mathrm{GS}\rangle = \prod_k [u_k - v_k a^\dagger(k)a^\dagger(k)]\,|0\rangle\,. \tag{22}$$

The maximum eigenvalue of $\partial_\Delta H$ corresponds to the fully occupied state in the picture of $b(k)$ and $b^\dagger(k)$, which we denote by $|\mathrm{FO}\rangle$ and can be written as

$$|\mathrm{FO}\rangle = \prod_k [u_k^* - v_k^* a(k)a(-k)]\,|\mathbb{1}\rangle\,. \tag{23}$$

One can explicitly check that $|\mathrm{FO}\rangle$ is normalized and satisfies $b^\dagger(k)\,|\mathrm{FO}\rangle = 0$ for all k. We call Eq. (23) the BCS-like fully occupied states since its construction is inspired by the BCS ground state. Thus, the optimal initial state for estimating Δ is

$$|\psi_0\rangle = (|\mathrm{GS}\rangle + |\mathrm{FO}\rangle)/\sqrt{2}. \tag{24}$$

A. HS for estimation of J and μ

The difference between the maximum and the minimum eigenvalues of $\partial_J H$ in the many-body Hilbert space is $|\cos k|$. Thus, the QFI for estimating J according to Eq. (5) is $I_0(J) = (\sum_k |\cos k|)^2 T^2$. In the limit $N\to\infty$,

$$I_0(J) = T^2[(N/2\pi)^2\int_0^{2\pi} dk|\cos k|]^2 = 4N^2T^2/\pi^2, \tag{25}$$

where we have replaced $\sum_k \to N/2\pi\int dk$ taking the continuum limit as the integrand is not singular in the integration region. In fact, the error introduced does not scale with N according to the analysis with the Euler-Maclaurin formula in Appendix B. Similarly, the difference between the maximum and the minimum eigenvalues of $\partial_\mu H$ in the many-body Hilbert space is 1 and, therefore, $I_0(\mu) = N^2T^2$. We see that the scaling of the ultimate QFI for estimating J and μ is the HS. The plot of $I_0(J)$ with the number of lattice sites is shown in Fig. 2. We will show shortly that even in the case of imperfect control or without control, such scaling is not altered.

B. HS to super-HS transition for estimating Δ

The maximum and minimum eigenvalues of $\partial_\Delta H$ in the many-body Hilbert space are $\gamma_\alpha(N)/2$ and 0, where

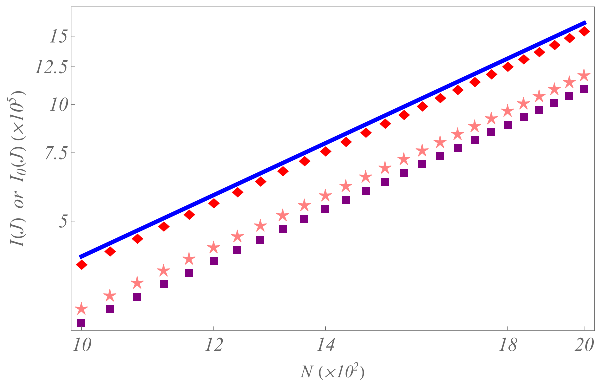

FIG. 2. Quantum Fisher information $I(J)$ for J estimation in the case with no control or imperfect control as well as for optimal control as a function of N for $\kappa_{l,\alpha} = l^{-\alpha}$. The blue solid line is the maximum possible QFI plotted according to the analytical expression Eq. (25) when optimal controls are applied where the long-range interaction terms are canceled (with probe time $T = 1$). All the discrete points are numerically calculated from Eq. (30). The values of the parameters are as follows: (i) red circle dots: $J = \mu = 10\Delta$ and $\alpha = 0$, (ii) pink stars are $J = \mu = \Delta$ and $\alpha = 0.5$, and (iii) purple squares: $J = \mu = \Delta$ and $\alpha = 0$.

$\gamma_\alpha(N) \equiv \sum_k |f_\alpha(k)|$. Thus, for estimating Δ, the QFI reads

$$I_0(\Delta) = [\gamma_\alpha(N)/2]^2 T^2. \tag{26}$$

Determining the scaling of $I_0(\Delta)$ boils down to computing the scaling of $\gamma_\alpha(N)$ at large N. Let us first discuss a simple case with $\kappa_{l,0} = 1$. In this case, $f_0(k) = \cot(k/2)$. According to Appendix C, when applying the Euler-Maclaurin formula, the upper bound of the scaling of the remainder, which is the difference between $\gamma_0(N)$ and the main integral $N/(2\pi)\int_{\pi/N}^{\pi}\cot(k/2)dk$, is N due to the singularity of $f_0(k)$ around $k = 0$. Nevertheless, since the main integral $N/(2\pi)\int_{\pi/N}^{\pi}\cot(k/2)dk \sim N \ln N$, which is still much larger than N in the asymptotic limit of larger N, we conclude that the leading order $\gamma_0(N)$ is N.

Let us next focus on the case of the power-law decay for the long-range interaction in the original proposal of LRK [23], i.e., $\kappa_{l,\alpha} = l^{-\alpha}$. For $\alpha > 1$, $f_\alpha(k)$ has no singularity for all the values of the momentum k. This is because $|\sum_{l=1}^{N-1}\sin(kl)/l^\alpha| \leqslant \sum_{l=1}^{N-1} 1/l^\alpha$ and the latter series is convergent for $\alpha > 1$. With the Euler-Maclaurin formula discussed in Appendix B, $\gamma_\alpha(N)$ scales as N. Thus, the QFI $I_0(\Delta)$ obeys the HS for $\alpha > 1$. For $0 < \alpha \leqslant 1$, using the properties of the polylogarithmic function [33], one finds $f_\alpha(k) \sim 1/k^{1-\alpha}$ (see also Appendix D and Ref. [23]). According to Appendix C, the upper bound of the scaling of the remainder in the Euler-Maclaurin formula is strictly slower than N, and the leading order of $\gamma_\alpha(N)$ is controlled by the main integral $N/2\pi\int_{\pi/N}^{\pi}|f_\alpha(k)|dk$. We note that $\int_{\pi/N}^{\pi}[|f_\alpha(k)| - 1/k^{1-\alpha}]dk$ should be constant as $N \to \infty$ since the singularity has been removed. So $\int_{\pi/N}^{\pi}|f_\alpha(k)|dk \sim \int_{\pi/N}^{\pi}1/k^{1-\alpha}dk$ is a constant, which does not scale with N and, therefore, $\gamma_\alpha(N) \sim N$. We, thus, find that for $\kappa_{l,\alpha} = l^{-\alpha}$, super-HS scaling only occurs for $\alpha = 0$.

Now, let us explore more general long-range interactions that satisfy the regularity condition at the beginning. As we have seen above, the scaling $\gamma_\alpha(N)$ crucially depends on the singularities of $f_\alpha(k)$, which is caused by the slow-decaying long-range interactions. We argue at the end of Appendix G that $\int_{1/N}^{\Lambda}dk f_\alpha(k) \sim N\int_1^N(\kappa_{x,\alpha}/x) \leqslant N \ln N$. Then according to Appendix C, we find the leading-order scaling of $\gamma_\alpha(N)$ is controlled by $N/2\pi\int_{1/N}^{\Lambda}dk f_\alpha(k) \sim N\int_1^N(\kappa_{x,\alpha}/x)dx$. We see that the maximum possible scaling $\gamma_\alpha(N)$ is $N \ln N$, where $\kappa_{x,\alpha}$ is a constant that does not depend on x. Therefore, according to Eq. (26),

$$I_0(\Delta) \sim N^2\left[\int_1^N(\kappa_{x,\alpha}/x)dx\right]^2, \tag{27}$$

and it is bounded by $N^2(\ln N)^2$ rather than the HS. In particular, when the long-range interaction decays sufficiently slow, $\int_1^N(\kappa_{x,\alpha}/x)$ can diverge at large N and, therefore, super-HS occurs for $I_0(\Delta)$. This is the case, e.g., when $\kappa_{x,\alpha} = [\ln(ex)]^{-\alpha} = (1 + \ln x)^{-\alpha}$ which satisfies the regularity conditions with $Q = 1$. So we obtain $\gamma_\alpha(N) \sim N\int_1^N dx/[x(1 + \ln x)^\alpha]$. The integral can be evaluated with the change of variable $s = 1 + \ln x$, which leads to

$$I_0(\Delta) \sim \begin{cases} N^2(\ln N)^{2(1-\alpha)}, & \alpha \in [0, 1), \\ N^2(\ln \ln N)^2, & \alpha = 1, \\ N^2, & \alpha > 1. \end{cases} \tag{28}$$

As a result, super-HS occurs for the very slow decay law dictated by the power of logarithms when $\alpha \leqslant 1$. As one can see from Figs. 3(a) and 3(b), the analytical scalings of $I_0(\Delta)$ for $\kappa_{l,0} = 1$ and $\kappa_{l,0.2} = (1 + \ln l)^{-0.2}$ shown by the blue solid lines, are in excellent agreement with their respective numerical calculations, shown by the cyan and red triangles in Figs. 3(a) and 3(b), respectively.

C. Resilience of the scaling under no or imperfect control

We have seen that the HS of $I_0(J)$ and $I_0(\mu)$ is due to the fact that the spectrum of $\mathscr{E}_J(k)$ and $\mathscr{E}_\mu(k)$ is regular near $k = 0$, whereas the possibility of super-HS scaling in $I_0(\Delta)$ is due to the fast divergence of $\mathscr{E}_\Delta(k)$ near $k = 0$. It is natural to consider the fate of these scaling laws when control is not optimally applied or is not available. To be more precise when the optimal control for estimating J or μ requires the exact cancellation of the long-range superconducting pairing term. The imperfect control for this case would be that this long-range interaction is not perfectly canceled, resulting in

$$H_\Delta + H_c = -\frac{J}{2}\sum_{j=1}^{N}(a_j^\dagger a_{j+1} + a_{j+1}^\dagger a_j) - \mu\sum_{j=1}^{N}\left(a_j^\dagger a_j - \frac{1}{2}\right) + \frac{(\Delta - \Delta_c)}{2}\sum_{j=1}^{N-1}\sum_{l=1}^{N-j}\kappa_{l,\alpha}(a_j a_{j+l} + a_{j+l}^\dagger a_j^\dagger), \tag{29}$$

where $\Delta_c \neq \Delta$. Similar concept also applies for the imperfect control for estimating Δ.

In these cases, according to Eq. (1), we find

$$I(\theta) = \left[\sum_k \mathscr{E}_\theta(k)\right]^2. \tag{30}$$

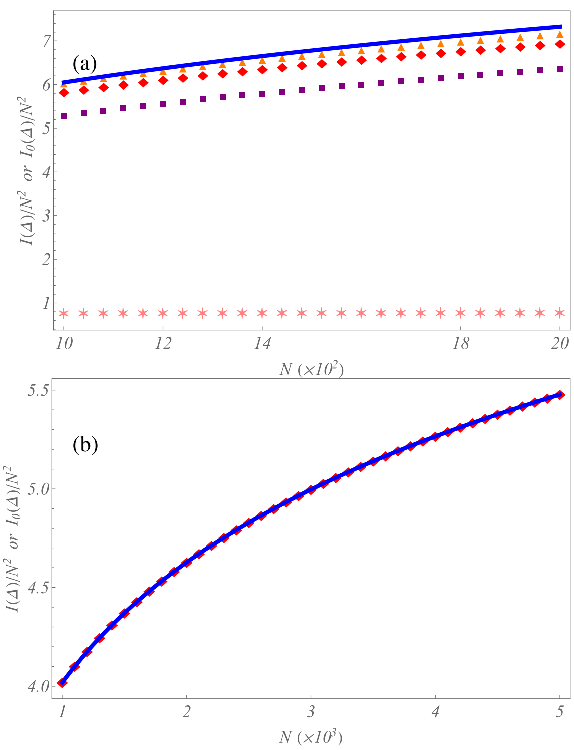

FIG. 3. Quantum Fisher information $I(\Delta)$ for Δ estimation in the case with no control or imperfect control as well as for optimal control as function of N for (a) $\kappa_{l,\alpha} = l^{-\alpha}$ and (b) $\kappa_{l,\alpha} = (1 + \ln l)^{-\alpha}$. The probe time $T = 1$ in both figures. (a) All the discrete points are numerically calculated from Eq. (30). The values of the parameters for: (i) red circle dots: $J = \mu = 0.5\Delta$ and $\alpha = 0$, (ii) purple squares: $J = \mu = \Delta$ and $\alpha = 0$, (iii) pink stars are $J = \mu = \Delta$ and $\alpha = 0.5$. (iv) Cyan triangles: $J = \mu = 0$ and $\alpha = 0$. The blue solid line is the scaling $N^2(\ln N)^2$ where the prefactor is determined by the QFI for $J = \mu = 0$ and $N = 1000$. (b) The red triangles are numerical calculations of $I_0(\Delta)$ for $\alpha = 0.2$, and the blue line is the fitted to the red triangles with $A(\ln N)^c + B$, where $A = 0.20$, $c = 1.54$ and $B = 0.17$. The values c is very close to the expected value $2(1 - \alpha) = 1.6$. The slight deviation of the scaling exponent between theory and the fitted results is because $\ln N$ is a very slowly increasing function compared to the power functions.

Let us first discuss the estimation of J. First, from Eqs. (8) and (12), one can readily obtain

$$\partial_J \epsilon_J(k) = \cos k(J \cos k + \mu)/\epsilon_J(k), \tag{31}$$

$$\xi_J(k) = \Delta f_\alpha(k) \cos k/\left[2\epsilon_J^2(k)\right]. \tag{32}$$

Since we focus on the no-control or imperfect control case $\Delta \neq 0$, we see that the only possibility for $\partial_J \epsilon_J(k)$ and $\partial_\mu \epsilon_\mu(k)$ to blow up is when their denominators vanish, i.e., $J \cos k + \mu = 0$ and $f_\alpha(k) = 0$ near $k = 0$. However, we note that whenever $f_\alpha(k) = 0$, $\partial_J \epsilon_J(k) = \pm \cos k$. The same argument also applies to $\xi_J(k)$. Therefore, $\mathscr{E}_J(k)$ does not blow up. Thus, we conclude in the absence of controls or in the presence of imperfect control, the HS is not affected. For the estimation of Δ, it is readily found from Eqs. (8) and (12) that

$$\partial_\Delta \epsilon_\Delta(k) = \Delta f_\alpha^2(k)/[4\epsilon_\Delta(k)], \tag{33}$$

$$\xi_\Delta(k) = -(J \cos k + \mu) f_\alpha(k)/\left[2\epsilon_\Delta^2(k)\right]. \tag{34}$$

Since around $k = 0$, $\epsilon_\Delta(k) \sim f_\alpha(k)$, we know $\lim_{k\to 0} \xi_\Delta(k) = 0$ and $\partial_\Delta \epsilon_\Delta(k) \sim f_\alpha(k)$. Therefore, the dominant divergence in $\mathscr{E}_\Delta(k)$ is controlled by $\partial_\Delta \epsilon_\Delta(k)$ and is the same as the case of the optimal estimation of Δ. The scaling of estimating Δ is again unchanged.

Figures 2 and 3 show a comparison between the cases with optimal controls and with no controls or imperfect controls, respectively. As we can see from these figures, the slopes of the lines for the cases with no or imperfect control match the one for optimal control. The same conclusion holds for the estimation of μ. Therefore, the role of optimal quantum controls here is to improve the prefactor of the leading-order scaling of the ultimate QFI rather than the scaling exponent.

IV. HIDDEN NONLINEARITY AND CONNECTION TO NONLINEAR METROLOGY

Super-HS scaling is well understood in parameter estimation of coupling constants of multibody spin operators in a Hamiltonian [20–22] describing multispin systems. Specifically, the upper bound of the scaling of the QFI in estimating the coupling constant of a l-body operator in many-body spin or qubit systems is N^{2l} [20–22]. One may, thus, wonder whether the scaling reported here for the superconducting strength Δ in the LRK model can be understood in view of these results. Even if the LRK is a linear model described by a quadratic Hamiltonian of Fermionic operators in $\{a_j, a_j^\dagger\}$, one may argue that it exhibits a hidden nonlinearity in the spin representation. The latter becomes apparent making use of the Jordan-Wigner transformation [34], which is highly nonlocal, in the sense that the transformation of two-body operators in the fermionic representation involves a string of Pauli operators in the spin representations. As shown in Appendix I, the explicit form of the LRK Hamiltonian in the spin representation reads

$$\begin{aligned} H_{\text{spin}} = &-\frac{J}{4}\sum_{j=1}^{N}\left(\sigma_j^x\sigma_{j+1}^x + \sigma_j^y\sigma_{j+1}^y\right) - \frac{\mu}{2}\sum_{j=1}^{N}\sigma_j^z \\ &- \frac{\Delta}{8}\sum_{j=1}^{N}\kappa_{1,\alpha}\left(\sigma_j^x\sigma_{j+1}^x - \sigma_j^y\sigma_{j+1}^y\right) \\ &+ \frac{\Delta}{8}\sum_{j=1}^{N}\sum_{l=2}^{N-1}(-1)^l\kappa_{l,\alpha}\left(\sigma_j^x\sigma_{j+l}^x - \sigma_j^y\sigma_{j+l}^y\right)\bigotimes_{k=1}^{l-1}\sigma_{j+k}^z. \end{aligned} \tag{35}$$

This representation makes explicit the fact that the long-range pairing term involves interaction among $(l + 1)$ spins with $1 \leqslant l \leqslant N - 1$. As a result, the scaling reported here for the LRK model agrees with the intuition that for spin systems, reaching the super-HS requires interactions involving more than one single spin operator [21,22]. Note, however, that in the spin representation the superconducting strength Δ does not couple solely to a single l-body operator term as in Refs. [21,22], it acts simultaneously as a coupling constant for a set of operators of varying rank l and norm with the latter being weighted by $\kappa_{l,\alpha}$. As a result, the scaling reported here does not readily follow from the super-HS known in quantum metrology. Rather, it generalizes nonlinear quantum metrology for parameter estimation of a coupling constant that couples simultaneously to multiple spin operators.

V. DISCUSSIONS AND CONCLUSIONS

We have established that the scaling of the QFI for estimating the superconducting strength Δ is bounded by $N^2(\ln N)^2$ rather than the HS due to the long-range interactions. As in Eq. (6), long-range interactions contain N^2 terms whose strength is controlled by $\kappa_{l,\alpha}$. Intuitively, if $\kappa_{l,\alpha}$ decays quickly, these N^2 terms effectively behave, such as a local interaction containing only N terms, such as in the estimation of J and μ and lead to the HS in estimating Δ. However, if $\kappa_{l,\alpha}$ decays sufficiently slow, these N^2 terms can collectively give rise to the super-HS behavior. We have illustrated this in two examples with $\kappa_{l,\alpha} = l^{-\alpha}$ and $\kappa_{l,\alpha} = (1 + \ln l)^{-\alpha}$, respectively. Interestingly, when N is not large enough, we have shown in Appendix H that super-HS $N^2(\ln N)^2$ and $N^2(\ln \ln N)^2$ can also occur as long as

$$\epsilon \ll (\ln N)^{-1} \tag{36}$$

for $\kappa_{x,\epsilon} = x^{-\epsilon}$ and

$$\epsilon \ll \ln \ln N \tag{37}$$

for $\kappa_{l,1+\epsilon} = (1 + \ln l)^{-(1+\epsilon)}$, respectively.

Note that the LRK model here is *linear* and, thus, different from the super-HS in the nonlinear models [20–22]. However, making use of the spin representation of the LRK model, we have shown that these results can be understood in the context of nonlinear quantum metrology regarding the parameter estimation of a coupling constant that simultaneously couples to a set of multispin operators of various ranks and norms.

Since the HS characterizes the many-body entanglement of the probes if the generator only contains local operators [13–15], our results may indicate there may be an intimate connection between the HS and the super-HS transition and the property of quantum entanglement. We have further shown that the singularity is not altered by whether external control is optimally applied or not. Therefore, we conclude that in the LRK model, quantum controls can improve the ultimate QFI by altering the prefactor whereas preserving the scaling exponent.

Our results are of direct relevance to practical quantum metrology with quantum dots [35], trapped ions [36,37], and cold atoms [38]. Our findings should be applicable to the relation between the HS/super-HS and the many-body entanglement [13–15], the physical preparations of the optimal initial states (fermionic GHZ states) [39], optimal detection associated with the HS, super-HS [4,40,41], and quantum estimation of the LRK in the presence of decoherence and dissipation [20].

ACKNOWLEDGMENTS

We thank H. Zhou for useful discussions. Part of this paper was performed when J.Y. visited S.P. at Sun Yat-Sen University (SYSU), China in May 2021. We thank SYSU for their warmth and hospitality. Support from the National Natural Science Foundation of China (NSFC) Grant No. 12075323, the NSF Grant No. DMR-1809343, and US Army Research Office Grant No. W911NF-18-10178 is greatly acknowledged.

APPENDIX A: THE DIAGONALIZATION OF THE LRK HAMILTONIAN AND THE GENERATOR FOR PARAMETER ESTIMATION

We note that the LKR Hamiltonian in momentum space reads [15]

$$\begin{aligned} H_\theta = & -\frac{J}{2}\sum_k [a^\dagger(k)a(k) + a^\dagger(-k)a(-k)]\cos k \\ & -\frac{\mu}{2}\left[\sum_k a^\dagger(k)a(k) + \sum_{-k} a^\dagger(-k)a(-k)\right] \\ & +\frac{i\Delta}{4}\sum_k [a(-k)a(-k) - a^\dagger(-k)a^\dagger(-k)]f_\alpha(k). \end{aligned} \tag{A1}$$

The Fourier transformation that relates the original Hamiltonian (6) to above Hamiltonian does not depend on any estimation parameters. Thus, the Fisher information is preserved by the transformation. Equation (A1) can be diagonalized as follows:

$$H_\theta = \frac{1}{2}\sum_k \epsilon_\theta(k)[a^\dagger(k), \quad a(-k)]U_\theta^\dagger(k)\sigma_z U_\theta(k)\begin{bmatrix} a(k) \\ a^\dagger(-k)\end{bmatrix}, \tag{A2}$$

through the Bogoliubov transformation $U_\theta(k)$,

$$U_\theta(k) \equiv \begin{pmatrix} \cos[\phi_\theta(k)/2] & i\sin[\phi_\theta(k)/2] \\ i\sin[\phi_\theta(k)/2] & \cos[\phi_\theta(k)/2]\end{pmatrix}, \tag{A3}$$

$$\sin\,\phi_\theta(k) = -\frac{\Delta}{2}\frac{f_\alpha(k)}{\epsilon_\theta(k)}, \tag{A4}$$

$$\cos\,\phi_\theta(k) = -\frac{(J\,\cos\,k + \mu)}{\epsilon_\theta(k)}. \tag{A5}$$

Denoting

$$\begin{bmatrix} \eta_\theta(k) \\ \eta_\theta^\dagger(-k)\end{bmatrix} \equiv U_\theta(k)\begin{bmatrix} a(k) \\ a^\dagger(-k)\end{bmatrix}, \tag{A6}$$

the Hamiltonian can be rewritten as

$$H_\theta = \sum_k \epsilon_\theta(k)\left[\eta_\theta^\dagger(k)\eta_\theta(k) - \frac{1}{2}\right]. \tag{A7}$$

The parameter-dependent constant $\sum_k \epsilon_\theta(k)/2$ does not contribute the Fisher information and will be suppressed. The generator for parameter estimation is [17,27]

$$G_\theta = \int_0^T \mathcal{U}_\theta^\dagger(\tau)\partial_\theta H_\theta \mathcal{U}_\theta(\tau)d\tau, \tag{A8}$$

where the evolution operator is $\mathcal{U}_\theta(\tau) = e^{-iH_\theta\tau}$. According to Eq. (A7), the generator contains two parts: The first part is due to the $\partial_\theta\epsilon_\theta(k)$, and the other is due to $\partial_\theta\eta_\theta^\dagger$ and $\partial_\theta\eta_\theta(k)$. It is readily found that

$$\begin{bmatrix}\partial_\theta\eta_\theta(k)\\ \partial_\theta\eta_\theta^\dagger(-k)\end{bmatrix} = \frac{d\phi_\theta}{d\theta}\left[\partial_\phi U_\theta(k)U_\theta^{-1}(k)\right]\begin{bmatrix}\eta_\theta(k)\\ \eta_\theta^\dagger(-k)\end{bmatrix} = \frac{i}{2}\frac{d\phi_\theta(k)}{d\theta}\sigma_x\begin{bmatrix}\eta_\theta(k)\\ \eta_\theta^\dagger(-k)\end{bmatrix} = -\frac{i\partial_\theta\cos\phi_\theta(k)}{2\sin\phi_\theta(k)}\sigma_x\begin{bmatrix}\eta_\theta(k)\\ \eta_\theta^\dagger(-k)\end{bmatrix}. \tag{A9}$$

Therefore,

$$\partial_\theta H_\theta = \sum_k \partial_\theta\epsilon_\theta(k)\eta_\theta^\dagger(k)\eta_\theta(k) + \frac{i}{2}\sum_k \xi_\theta(k)\epsilon_\theta(k)[\eta_\theta(-k)\eta_\theta(k) - \eta_\theta^\dagger(k)\eta_\theta^\dagger(-k)]. \tag{A10}$$

Substituting Eq. (A10) into Eq. (A8), we find

$$\begin{aligned}G_\theta = {}& T\sum_k \partial_\theta\epsilon_\theta(k)\eta_\theta^\dagger(k)\eta_\theta(k) + \frac{i}{2}\sum_k \xi_\theta(k)\epsilon_\theta(k)\int_0^T d\tau\,\exp\left[i\sum_p \epsilon_\theta(p)\eta_\theta^\dagger(p)\eta_\theta(p)\tau\right]\\ &\times[\eta_\theta(-k)\eta_\theta(k) - \eta_\theta^\dagger(k)\eta_\theta^\dagger(-k)]\exp\left[-i\sum_{p'}\epsilon_\theta(p')\eta_\theta^\dagger(p')\eta_\theta(p')\tau\right].\end{aligned} \tag{A11}$$

Note that the product of two fermionic creation and annihilation operators behaves like a c number when commuting with fermionic operators in other modes. We further note that the negative modes are equivalent to the positive modes via the identification $-k \sim 2\pi - k$. With these two observations, it is readily checked that

$$\begin{aligned}&\exp\left[i\sum_p \epsilon_\theta(p)\eta_\theta^\dagger(p)\eta_\theta(p)\tau\right][\eta_\theta(-k)\eta_\theta(k) - \eta_\theta^\dagger(k)\eta_\theta^\dagger(-k)]\exp\left[-i\sum_{p'}\epsilon_\theta(p')\eta_\theta^\dagger(p')\eta_\theta(p')\tau\right]\\ &= \exp\{i[\epsilon_\theta(k)\eta_\theta^\dagger(k)\eta_\theta(k) + \epsilon_\theta(2\pi-k)\eta_\theta^\dagger(2\pi-k)\eta_\theta(2\pi-k)]\tau\}[\eta_\theta(-k)\eta_\theta(k) - \eta_\theta^\dagger(k)\eta_\theta^\dagger(-k)]\\ &\quad\times e^{-i[\epsilon_\theta(k)\eta_\theta^\dagger(k)\eta_\theta(k)+\epsilon_\theta(2\pi-k)\eta_\theta^\dagger(2\pi-k)\eta_\theta(2\pi-k)]\tau}\\ &= e^{i\epsilon_\theta(k)\tau[\eta_\theta^\dagger(k)\eta_\theta(k)+\eta_\theta^\dagger(-k)\eta_\theta(-k)]}[\eta_\theta(-k)\eta_\theta(k) - \eta_\theta^\dagger(k)\eta_\theta^\dagger(-k)]e^{-i\epsilon_\theta(k)\tau[\eta_\theta^\dagger(k)\eta_\theta(k)+\eta_\theta^\dagger(-k)\eta_\theta(-k)]}.\end{aligned} \tag{A12}$$

Using the relation,

$$e^{i\theta\eta^\dagger\eta} = 1 + \eta^\dagger\eta(e^{i\theta}-1) = e^{i\theta} - \eta\eta^\dagger(e^{i\theta}-1) \tag{A13}$$

for fermionic operators, Eq. (A12) becomes

$$\begin{aligned}&e^{i\epsilon_\theta(k)\tau[\eta_\theta^\dagger(k)\eta_\theta(k)+\eta_\theta^\dagger(-k)\eta_\theta(-k)]}\eta_\theta(-k)\eta_\theta(k)e^{-i\epsilon_\theta(k)\tau[\eta_\theta^\dagger(k)\eta_\theta(k)+\eta_\theta^\dagger(-k)\eta_\theta(-k)]}\\ &= [1+\eta_\theta^\dagger(k)\eta_\theta(k)(e^{i\epsilon_\theta(k)\tau}-1)][1+\eta_\theta^\dagger(-k)\eta_\theta(-k)(e^{i\epsilon_\theta(k)\tau}-1)]\eta_\theta(-k)\eta_\theta(k)\\ &\quad\times[e^{-i\epsilon_\theta(k)\tau} - \eta_\theta(k)\eta_\theta^\dagger(k)(e^{-i\epsilon_\theta(k)\tau}-1)][e^{-i\epsilon_\theta(k)\tau} - \eta_\theta(-k)\eta_\theta^\dagger(-k)(e^{-i\epsilon_\theta(k)\tau}-1)]\\ &= e^{-i\epsilon_\theta(k)\tau}[1+\eta_\theta^\dagger(k)\eta_\theta(k)(e^{i\epsilon_\theta(k)\tau}-1)]\eta_\theta(-k)\eta_\theta(k)[e^{-i\epsilon_\theta(k)\tau} - \eta_\theta(-k)\eta_\theta^\dagger(-k)(e^{-i\epsilon_\theta(k)\tau}-1)]\\ &= -e^{-i\epsilon_\theta(k)\tau}[1+\eta_\theta^\dagger(k)\eta_\theta(k)(e^{i\epsilon_\theta(k)\tau}-1)]\eta_\theta(k)\eta_\theta(-k)[e^{-i\epsilon_\theta(k)\tau} - \eta_\theta(-k)\eta_\theta^\dagger(-k)(e^{-i\epsilon_\theta(k)\tau}-1)]\\ &= -e^{-2i\epsilon_\theta(k)\tau}\eta_\theta(k)\eta_\theta(-k)\\ &= e^{-2i\epsilon_\theta(k)\tau}\eta_\theta(-k)\eta_\theta(k),\end{aligned} \tag{A14}$$

where we have used $\eta_\theta^2(-k) = \eta_\theta^2(k) = 0$. The generator now becomes

$$G_\theta = \sum_k\left\{T\partial_\theta\epsilon_\theta(k)\eta_\theta^\dagger(k)\eta_\theta(k) + \frac{\xi_\theta(k)}{4}\{(1-e^{-2i\epsilon_\theta(k)T})\eta_\theta(-k)\eta_\theta(k) + [1-e^{2i\epsilon_\theta(k)T})]\eta_\theta^\dagger(k)\eta_\theta^\dagger(-k)\}\right\}. \tag{A15}$$

We rewrite Eq. (A15) in a more compact form

$$G_\theta = \frac{1}{2}\sum_k[\eta_\theta^\dagger(k),\quad \eta_\theta(-k)]\mathscr{G}_\theta(k)\begin{bmatrix}\eta_\theta(k)\\ \eta_\theta^\dagger(-k)\end{bmatrix}, \tag{A16}$$

where the matrix $\mathscr{G}_\theta(k)$ is defined as

$$\mathscr{G}_\theta(k) \equiv T\partial_\theta\epsilon_\theta(k)\sigma_z + \frac{\xi_\theta(k)}{2}\{1-\cos[2\epsilon_\theta(k)T]\}\sigma_x + \frac{\xi_\theta(k)}{2}\sin[2\epsilon_\theta(k)T]\sigma_y = \mathscr{E}_\theta(k)\boldsymbol{n}_\theta(k)\cdot\boldsymbol{\sigma}. \tag{A17}$$

Furthermore, we note that

$$V_\theta^\dagger(k)[\boldsymbol{n}_\theta(k)\cdot\boldsymbol{\sigma}]V_\theta(k)=\sigma_z, \tag{A18}$$

where

$$V_\theta(k)=(|\uparrow_{\boldsymbol{n}_\theta(k)}\rangle\,,\quad |\downarrow_{\boldsymbol{n}_\theta(k)}\rangle), \tag{A19}$$

and $|\uparrow_{\boldsymbol{n}_\theta(k)}\rangle$ and $|\downarrow_{\boldsymbol{n}_\theta(k)}\rangle$ are the vectors aligned and antialigned with vector $\boldsymbol{n}_\theta(k)$ on the Bloch sphere, respectively. Introducing,

$$\begin{bmatrix}\psi_\theta(k)\\ \psi^\dagger(-k)\end{bmatrix}\equiv V_\theta(k)\begin{bmatrix}\eta_\theta(k)\\ \eta^\dagger(-k)\end{bmatrix}, \tag{A20}$$

one can readily obtain Eqs. (10) and (11) in the main text.

APPENDIX B: THE EULER-MACLAURIN FORMULA

Lemma 1. (Euler-Maclaurin formula) For arbitrary function $g(x)$ with continuous derivatives, the infinite series $\sum_{n=a}^{b} g(m)$ can be converted to the corresponding integral plus remainder terms via the Euler-Maclaurin formula [42],

$$\sum_{n=a}^{n=b} g(n)=\int_a^b g(x)dx+R, \tag{B1}$$

where the remainder is

$$R=\frac{1}{2}[g(b)-g(a)]+\sum_{m=1}^{M}\frac{b_{2m}}{(2m)!}[g^{(2m-1)}(b)-g^{(2m-1)}(a)]$$
$$+\int_a^b\frac{1}{(2M+1)!}P_{2M+1}(x)g^{(2M+1)}(x)dx. \tag{B2}$$

Here, M can be arbitrarily chosen from the natural numbers 0–2, ..., b_{2m} is the Bernoulli number. $P_0(x)=1$ for $M>0$,

$$P_M(x)=\frac{1}{M!}B_M(\{x\}), \tag{B3}$$

where$\{x\}\equiv x-[x]$ and B_M is the Bernoulli polynomial.

We can use the Euler-Maclaurin formula to approximate a series,

$$\sum_{n=a}^{b} f\left(\frac{(2n+1)\pi}{N}\right)=\sum_{k=k_a}^{k_b} f(k), \tag{B4}$$

where we have $k=(2n+1)\pi/N$. We assume $f(k)$ is piecewise smooth on $[k_a,k_b]$ and does not blow up on $[k_a,k_b]$. *We allow some discontinuities in the first derivatives if $M=1$ so that $f(k)$ may contain an absolute value or a square root.* Without loss of generality, we can assume $f(k)$ is smooth on interval F_j's where $\cup_j F_j=[k_a,k_b]$. When denoting the function in terms of the variable, these intervals are denoted as E_j's. Applying the Euler-Maclaurin formula for these intervals, respectively, with $M=0$, we find

$$\sum_{n=0}^{N-1} f\left[\frac{(2n+1)\pi}{N}\right]=\sum_j\left\{\int_{E_j} f\left[\frac{(2x+1)\pi}{N}\right]dx+R_j\right\}, \tag{B5}$$

where

$$R_j=\frac{2\pi}{N}\int_{E_j}P_1(x)\sin\left[\frac{(2x+1)\pi}{N}\right]dx+\text{boundary terms}, \tag{B6}$$

and $P_1(x)$ is defined in Eq. (B3). We note that the boundary terms remain finite and do not scale with N. They will be omitted subsequently. In the Fourier representation, we find

$$\sum_{n=0}^{N-1} f\left(\frac{[2n+1]\pi}{N}\right)=\frac{N}{2\pi}\int_{\pi/N}^{2\pi-\pi/N} f(k)dk+\sum_j R_j, \tag{B7}$$

where

$$R_j=\int_{F_j}P_1\left(\frac{Nk}{2\pi}-\frac{1}{2}\right)f'(k)dk. \tag{B8}$$

Since $f(k)$ is differentiable on F_j, $f'(k)$ is regular on F_j. On the other hand, $P_1(x)\in[-1/2,1/2]$ is bounded. We find that R_j remains finite as long as the number of the F_j's does not scale with N. *So we conclude that when $f(k)$ is regular,* $\sum_{k=k_a}^{k=k_b} f(k)\sim N$. For example, in Eq. (25) of the main text, we take $f(k)=|\cos k|$, which is differentiable on $F_1=[\pi/N,\pi/2-\pi/N]$, $F_2=[\pi/2+\pi/N,3\pi/2-\pi/N]$, and $F_3=[3\pi/2+\pi/N,2\pi-\pi/N]$, respectively.

However, we note that if $f(k)$ has a singularity in $[0,2\pi]$, the remainder may not necessarily stay as a constant as $N\to\infty$. For example, if we take

$$f(k)=\cot\left[\frac{k}{2}\right], \tag{B9}$$

where $k\in[\pi/N,\pi-\pi/N]$, then we obtain

$$\sum_{n=0}^{N/2-1}\cot\left[\frac{(2n+1)\pi}{2N}\right]=\frac{N}{\pi}\int_{\pi/N}^{\pi-\pi/N}\cot\left(\frac{k}{2}\right)dk+R, \tag{B10}$$

where

$$R=\frac{1}{2}\left[\cot\left(\frac{\pi}{2}-\frac{\pi}{2N}\right)-\cot\left(\frac{\pi}{2N}\right)\right]$$
$$-\int_{\pi/N}^{\pi-\pi/N}P_1\left(\frac{Nk}{2\pi}-\frac{1}{2}\right)\frac{1}{\sin^2(k/2)}dk, \tag{B11}$$

with $P_1(t)$ given in Eq. (B3). The integrand in the remainder has a singularity around $k=0$, and there the main integral is no longer a good approximation of the sum. Nevertheless, we can upper bound the scaling of the integral in the remainder, i.e.,

$$\left|\int_{\pi/N}^{\pi-\pi/N}P_1\left(\frac{Nk}{2\pi}-\frac{1}{2}\right)\frac{1}{\sin^2(k/2)}dk\right|$$
$$\leqslant\int_{\pi/N}^{\pi-\pi/N}\frac{1}{\sin^2(k/2)}\sim\cot\left(\frac{\pi}{2N}\right). \tag{B12}$$

We, thus, conclude the remainder will scale at most as N. Since $\int_{\pi/N}^{\pi-\pi/N}\cot(k/2)dk\sim N\ln N$, we obtain the scaling of $\gamma_0(N)$ in the main text. We see that in the current case the remainder depends on N instead of being a constant as indicated in Eq. (B12). We would like to emphasize that *when the summand of a sum has a singularity in the limit $N\to\infty$; it is not rigorous to analyze the scaling of the sum only with the main integral because the remainder may contribute to the scaling.*

APPENDIX C: THE SCALING OF $\gamma_\alpha(N)$ FOR $f_\alpha(k) \leqslant O(1/k)$ NEAR $k = 0$

Theorem 1. We will assume the only possible singularity of $f_\alpha(k)$ is near $k = 0$, a fact which we will prove in Corollary 1. Then the scaling of $\gamma_\alpha(N)$ is controlled by the main integral if $f_\alpha(k) \leqslant O(1/k)$ near $k = 0$.

Proof. Let us first focus on the case $f_\alpha(k)$ is strictly slower than $1/k$ near $k = 0$. We denote E_j as the intervals where $f_\alpha([2x+1]\pi/N)$ is as smooth as function x. Similar as in Appendix B, this denomination allows $f_\alpha(k)$ to be piecewise functions joined by smooth functions, as long as there are no singularities at the joints. The intervals $E_j$become F_j when the function is written in terms of the variable k. In particular, one can easily show that $f_\alpha(\pi/N)$ is positive. Applying Euler-Maclaurin formula (B1) to each of these intervals, we find

$$\gamma_\alpha(N) = 2\sum_j \left[\int_{E_j} (-1)^{j-1} f_\alpha\left(\frac{[2x+1]\pi}{N}\right)dx + R_{\alpha j}\right], \tag{C1}$$

where the remainder is

$$R_{\alpha j} = \int_{E_j} P_1(x)(-1)^{j-1} f'\left(\frac{[2n+1]x\pi}{N}\right)dx + \text{boundary terms}. \tag{C2}$$

Since the boundary terms do not scale with N, we will suppress them in subsequent analysis. Now we change x back to k, and we find

$$\gamma_\alpha(N) = 2\left[\frac{N}{2\pi}\int_{\pi/N}^{\pi-\pi/N} |f_\alpha(k)|dk + \sum_j R_{\alpha j}\right], \tag{C3}$$

where

$$R_{\alpha j} = \int_{F_j} P_1\left(\frac{Nk}{2\pi} - \frac{1}{2}\right)(-1)^{j-1} f'_\alpha(k)dk. \tag{C4}$$

For the remainders, if F_j does not contain the origin, then the integral in R_j is regular and does not scale with the constant. For F_j contains the origin, we use a common trick in asymptotic analysis [43]: The leading order of a singular integral can be found by replacing the integrand with its leading-order Laurent expansion near the singular point. In our current case, since

$$f_\alpha(k) < O\left(\frac{1}{k}\right), \tag{C5}$$

we find

$$\begin{aligned}
&\left|\int_{F_j} P_1\left(\frac{Nk}{2\pi} - \frac{1}{2}\right)(-1)^{j-1} f'_\alpha(k)dk\right| \\
&< \left|\int_{F_j} P_1\left(\frac{Nk}{2\pi} - \frac{1}{2}\right)(-1)^{j-1}\left(\frac{1}{k}\right)' dk\right| \\
&\leqslant \left|\int_{\pi/N}\left(\frac{1}{k}\right)' dk\right| \sim N,
\end{aligned} \tag{C6}$$

where we have used that $P_1(x) \in [-1/2, 1/2]$ is bounded. That is, the remainder scale scales strictly slower than N, which is subleading order compared to the first term on the right-hand side of Eq. (C3).

When $f_\alpha(k) \sim O(1/k)$, one can go through the same argument and will find that the main integral will scale as $N \ln N$ whereas the upper bound of the scaling of the remainder is N. Therefore, we conclude that the leading-order scaling of $\gamma_\alpha(N)$ is only given by the main integral if $f_\alpha(k) \leqslant O(1/k)$ near $k = 0$. We conclude this Appendix by noting that the condition $f_\alpha(k) \leqslant O(1/k)$ is nontrivial and essential: *Had $f_\alpha(k)$ scaled as $1/k^{1+\varepsilon}$ near $k = 0$, where ε is an arbitrary positive number, the above proof would yield that both the main integral and the upper bound of the remainder $R_{\alpha j}$ scales $N^{1+\varepsilon}$*. The analysis of the scaling of $\gamma_\alpha(N)$ would be subtle because the leading-order scaling of the main integral and the remainder $R_{\alpha j}$ might cancel each other. Fortunately, we see such a situation does not occur because we have shown in the main text that $f_\alpha(k) \leqslant O(1/k)$.

APPENDIX D: THE SINGULARITY OF $f_\alpha(k)$ FOR $\kappa_{l,\alpha} = l^{-\alpha}$ WITH $\alpha \in (0, 1]$

In this Appendix, we prove an analytic property of $f_\alpha(k)$ for the particular case where $\kappa_{l,\alpha} = l^{-\alpha}$,

$$f_\alpha(k) \sim \frac{1}{k^{1-\alpha}}, \quad \alpha \in (0, 1]. \tag{D1}$$

This result can be shown using the singularity of the polylogarithm functions [23,33]. However, this approach does not allow to obtain the general property of $f_\alpha(k)$ when $\kappa_{l,\alpha}$ takes a more general class of functions. Now we will explicitly show the singularity of $f_\alpha(k) \sim 1/k^{1-\alpha}$ around $k = 0$ for $\alpha \in (0, 1]$ without resorting to the polylogarithm functions. Recall

$$f_\alpha(k) \equiv 2\sum_{l=1}^{N/2-1} \kappa_{l,\alpha}\sin(kl) + \kappa_{N/2,\alpha}. \tag{D2}$$

Note that due to the regularity condition (E1), we know that $\kappa_{N/2,\alpha}$ is finite as $N \to \infty$. Therefore, in what follows we will omit $\kappa_{N/2,\alpha}$ in the definition of $f_\alpha(k)$ because it does not affect the analytic property of $f_\alpha(k)$. Now we are in a position to prove Eq. (D1):

Proof. Apparently $f_0(k)$ can be exactly calculated to be $\cot(k/2)$ which scales as $1/k$ near $k = 0$. For the case of $\alpha \in (0, 1]$, after applying the Euler-Maclaurin formula (B1), $f_\alpha(k)$ becomes

$$f_\alpha(k) = 2\mathscr{F}_\alpha(k) + \mathscr{R}_\alpha(k), \tag{D3}$$

where

$$\mathscr{F}_\alpha(k) = \int_1^{N/2-1} \frac{\sin(kx)}{x^\alpha}dx, \tag{D4}$$

and the remainder is

$$\mathscr{R}_\alpha(k) = 2k\int_1^N P_1(\{x\})\frac{\cos(kx)}{x^\alpha} - 2\int_1^N P_1(\{x\})\frac{\sin(kx)}{x^{\alpha+1}}, \tag{D5}$$

where we have again ignored the finite boundary terms. Apparently the second term in Eq. (D5) is finite and, therefore, will not contribute to the singularity of $f_\alpha(k)$ since

$$2\left|\int_1^N P_1(\{x\})\frac{\sin(kx)}{x^{\alpha+1}}\right| < \left|\int_1^N \frac{1}{x^{\alpha+1}}\right| < \infty. \tag{D6}$$

Our goal now is to determine the asymptotic behavior of the first term of Eq. (D5). Applying Fourier transform of $P_1(\{x\})$ [42],

$$P_1(\{x\}) = -\sum_{m=1}^{\infty} \frac{\sin(2m\pi x)}{m\pi}, \tag{D7}$$

we obtain

$$\int_1^N P_1(\{x\}) \frac{\cos(kx)}{x^\alpha} dx = -\frac{1}{2}\sum_{m=1}^{\infty}\frac{1}{m\pi}\int_1^N \left\{\frac{\sin[(2m\pi+k)x]}{x^\alpha} + \frac{\sin[(2m\pi-k)x]}{x^\alpha}\right\} dx. \tag{D8}$$

Integrating by parts, we find that

$$\int_1^N \frac{\sin[(2m\pi+k)x]}{x^\alpha} = \frac{1}{2m\pi+k}\left\{\frac{\cos[(2m\pi+k)x]}{x^\alpha}\Big|_{x=1}^{N} + \alpha\int_1^N \frac{\cos[(2m\pi+k)x]}{x^{\alpha+1}} dx\right\}. \tag{D9}$$

Apparently, the integral on the right-hand side is bounded in the limit $N \to \infty$ as long as $\alpha > 0$. So in the limit $N \to \infty$, we find

$$\int_1^N \frac{\sin[(2m\pi+k)x]}{x^\alpha} \lesssim \frac{1}{2m\pi+k}. \tag{D10}$$

By similar argument, one can show

$$\int_1^N \frac{\sin[(2m\pi-k)x]}{x^\alpha} \lesssim \frac{1}{2m\pi-k}. \tag{D11}$$

Note if k is resonant with $2m\pi$ then the original integral vanishes, and there is no need to do the scaling analysis for the second integral on the right-hand side of Eq. (D8). Substituting the above results into Eq. (D8), we find

$$\int_1^N P_1(\{x\}) \frac{\cos(kx)}{x^\alpha} \lesssim \sum_{m=1}^{\infty}\frac{1}{m^2} < \infty. \tag{D12}$$

Up to now, we have shown that there is no singularity in the remainder as long as $\alpha > 0$. To see the singularity in the first term of Eq. (D3), we perform a change in variables $kl = s$ and obtain

$$\mathscr{F}_\alpha(k) = \frac{1}{k^{1-\alpha}}\int_k^{n\pi+\pi/2} \frac{\sin s}{s^\alpha} ds, \tag{D13}$$

where we note $Nk = (2n+1)\pi$, where $n = 0, 1, \ldots, N-1$. In the limit $N \to \infty$, if finite n is finite, apparently the singularity of $f_\alpha(k) \sim 1/k^{1-\alpha}$. On the other hand, if $n \to \infty$, the integral in Eq. (D13) is still finite since

$$\int_0^\infty ds \frac{\sin s}{s^\alpha} = \Gamma(1-\alpha)\cos\left(\frac{\pi\alpha}{2}\right) \quad \text{for } \alpha \in (0, 1], \tag{D14}$$

as we will now show. We note that

$$\lim_{n\to\infty}\int_0^{n\pi+\pi/2} \frac{\sin s}{s^\alpha} ds = \int_0^\infty ds \frac{\sin s}{s^\alpha} = \text{Im}\int_0^\infty ds\, s^{-\alpha} e^{is}. \tag{D15}$$

One can evaluate Eq. (D15) by first replacing $s \to it$ and obtain

$$\int_0^\infty ds\, s^{-\alpha}e^{is} = i^{1-\alpha}\int_0^{i\infty} dt\, t^{-\alpha}e^{-t} = i^{1-\alpha}\lim_{\varepsilon\to 0}\left[\int_0^{i\varepsilon} dt\, t^{-\alpha}e^{-t} + \int_{i\varepsilon}^{i\infty} dt\, t^{-\alpha}e^{-t}\right]. \tag{D16}$$

The convergence of the first integral on the right-hand side of Eq. (D16) requires that $\alpha < 1$. The convergence of the second integral on the right-hand side of Eq. (D16) requires the integrand vanishes at $t = i\infty$, which leads to $\alpha > 0$. Now we take advantage of the analyticity of the integrand for $\alpha \in (0, 1]$ and rotate the integral from the positive imaginary t axis to the positive real t axis, which yields

$$\int_0^{i\infty} dt\, t^{-\alpha}e^{-t} = \int_0^\infty dt\, t^{-\alpha}e^{-t} = \Gamma(1-\alpha), \tag{D17}$$

which concludes the proof of Eq. (D14) for $\alpha \in (0, 1)$. In fact Eq. (D14) also holds for $\alpha = 1$ since $\int_0^\infty ds \sin s/s = \frac{\pi}{2}$ which can be evaluated by the residue theorem is actually $\lim_{\alpha\to 1}\Gamma(1-\alpha)\cos(\frac{\pi\alpha}{2})$.

Therefore, we have successfully shown that the singularity of $f_\alpha(k)$ only lies in the main term of the Euler-Maclaurin formula, which is Eq. (D3).

APPENDIX E: AN INTEGRAL APPROXIMATION TO $f_\alpha(k)$

We show in Appendix D that the singularity of $f_\alpha(k)$ when $\kappa_{l,\alpha} = l^{-\alpha}$ can be explicitly found with only elementary techniques, without resorting to the polylogarithmic function as in the original proposal of the LRK [23]. The advantage of this approach is that it allows us to prove the following theorem for general functions $\kappa_{l,\alpha}$ that satisfy the regularity conditions (E1) and (E2):

Theorem 2. We consider a general piecewise smooth function $\kappa_{x,\alpha}$ that satisfies the regularity conditions in the main text, i.e., $\kappa_{x,\alpha}$ satisfies: (i)

$$\left|\kappa_{x,\alpha}^{(q)}\right| < \infty, \quad q = 0, 1, \ldots, 2Q, \tag{E1}$$

which holds piecewisely on $[1, \infty]$, and
(ii)

$$\left|\int_1^\infty \kappa_{x,\alpha}^{(2Q+1)} dx\right| < \infty, \tag{E2}$$

where Q is a non-negative integer and the superscript (q) denotes the qth derivative with respect to x.

Then the singularity of $f_\alpha(k)$ near $k = 0$ is controlled by the main integral in the Euler-Maclaurin formula, i.e., the first term in

$$f_\alpha(k) = 2\mathscr{F}_\alpha(k) + \mathscr{R}_\alpha(k). \tag{E3}$$

Before we start the proof, let us first note that for the long-range decay function $d_{x,\alpha}$, we allow not only smooth functions of x, but also piecewise functions consisting of several smooth functions. This is because, as we have seen in Appendices B and C, one can apply the Euler-Maclaurin in a piecewise way. The condition (E1) indicates there can be only discontinuities at the joints, but no singularities. Nevertheless, in what follows, we will prove for the case when $d_{x,\alpha}$ is smooth $[1,\infty]$, which can be easily generalized to the case of piecewise smoothness without any difficulty.

Proof. We take $M = Q$ in the Euler-Maclaurin formula (B1), and obtain

$$f_\alpha(k) = 2\mathscr{F}_\alpha(k) + \mathscr{R}_\alpha(k), \tag{E4}$$

where

$$\mathscr{F}_\alpha(k) = \int_1^{N/2-1} \sin(kx)\kappa_{x,\alpha}dx, \tag{E5}$$

$$\mathscr{R}_\alpha(k) = \sum_{q=0}^{2Q+1}\mathscr{R}_{\alpha,q}(k) + \sum_{m=1}^{Q}\frac{b_{2m}}{(2m)!}[\sin(kx)\kappa_{x,\alpha}]^{(2m-1)}\Big|_{x=1}^{x=N/2-1}, \tag{E6}$$

$$\mathscr{R}_{\alpha,\,q}(k) \equiv \mathcal{C}_{Q,q}\int_1^{N/2-1} P_{2Q+1}(x)[\sin(kx)]^{(q)}[\kappa_{x,\alpha}]^{(2Q+1-q)}dx, \tag{E7}$$

$$\mathcal{C}_{Q,\,q} \equiv \binom{2Q-1}{q}\frac{1}{(2Q+1)!}. \tag{E8}$$

Apparently, the boundary term is finite due to the regularity condition (E1). Thus, we will focus on the integral in the remainder $\mathscr{R}_\alpha(k)$ subsequently. For $q = 0$, we find

$$\mathscr{R}_{\alpha,q}(k) \leqslant \mathcal{C}_{Q,q}\mathcal{C}_{2Q+1}\left|\int_1^{N/2-1}\kappa_{x,\alpha}^{(2Q+1)}dx\right| < \infty, \tag{E9}$$

where we have used the fact that $P_{2Q+1}(x)$ is bounded, $|P_{2Q+1}(x)| \leqslant \mathcal{C}_{2Q+1}$ and Eq. (E2). When $q \geqslant 1$, we apply the Fourier transform of $P_{2Q+1}(x)$ [42],

$$P_{2Q+1}(x) = \sum_{m=1}^{\infty}(-1)^{Q-1}\frac{2\sin(2m\pi x)}{(2m\pi)^{2Q+1}}. \tag{E10}$$

to Eq. (E7). For r even $q > 0$, we obtain

$$\mathscr{R}_{\alpha,q}(k) = \mathcal{C}_{Q,q}k^q(-1)^{Q-1+q/2}\sum_{m=1}^{\infty}\frac{1}{(2m\pi)^{2Q+1}}\int_1^{N/2-1}\{\cos[(2m\pi - k)x] - \cos[(2m\pi + k)x]\}\kappa_{x,\alpha}^{(2Q+1-q)}dx, \tag{E11}$$

and for odd $q \geqslant 1$, we obtain

$$\mathscr{R}_{\alpha,q}(k) = \mathcal{C}_{Q,q}k^q(-1)^{Q-1+(q-1)/2}\sum_{m=1}^{\infty}\frac{1}{(2m\pi)^{2Q+1}}\int_1^{N/2-1}\{\sin[(2m\pi + k)x] + \sin[(2m\pi - k)x]\}\kappa_{x,\alpha}^{(2Q+1-q)}dx. \tag{E12}$$

Since the convergence of the series is determined by the behavior of the general term at large values of the index, we will focus on the case of large m in the series in Eqs. (E11) and (E12) subsequently. Similarly with Eqs. (D9)–(D12), one can perform integration by parts until one gets an integrand that contains $(\kappa_{x,\,\alpha})^{(2Q+1)}$, which yields

$$\begin{aligned}\int_1^{N/2-1}\cos[(2m\pi \pm k)x](\kappa_{x,\alpha})^{(2Q+1-q)}dx = \frac{1}{(2m\pi \pm k)}\Bigg\{&\sin[(2m\pi \pm k)x](\kappa_{x,\alpha})^{(2Q+1-q)}\Big|_{x=1}^{x=\infty}\\ &+\frac{1}{(2m\pi \pm k)}\Big[\cos[(2m\pi \pm k)x](\kappa_{x,\,\alpha})^{(2Q+2-q)}|_{x=1}^{x=\infty}\Big] + \cdots\Bigg\}\\ &+\frac{(-1)^{(q-1)/2}}{(2m\pi \pm k)^q}\int_1^{N/2-1}\cos[(2m\pi \pm k)x]\kappa_{x,\alpha}^{(2Q+1)}dx,\end{aligned} \tag{E13}$$

Apparently the last integral is bounded, according to Eq. (E2). Therefore, for large m we know

$$\left|\int_1^{N/2-1}\cos[(2m\pi \pm k)x](\kappa_{x,\alpha})^{(2Q+1-q)}dx\right| \lesssim \frac{\mathcal{C}_{2Q+1-q}(\alpha)}{(2m\pi \pm k)}, \tag{E14}$$

where

$$\mathcal{C}_q(\alpha) \equiv \left|\left(\kappa_{x,\alpha}^{(q)}\right)_{x=1}\right| + \left|\left(\kappa_{x,\alpha}^{(q)}\right)_{x=\infty}\right|, \tag{E15}$$

which is finite according to the regularity condition Eq. (E1). With sa imilar argument, we obtain

$$\left|\int_1^{N/2-1}\sin[(2m\pi \pm k)x]\kappa_{x,\alpha}^{(2Q+1-q)}dx\right| \lesssim \frac{\mathcal{C}_{2Q+1-q}(\alpha)}{(2m\pi \pm k)} \tag{E16}$$

for large m. So we conclude

$$|\mathscr{R}_{\alpha,q}(k)| \lesssim \mathcal{C}_{Q,q}\mathcal{C}_{2Q+1-q}(\alpha)k^q\sum_{m=1}^{\infty}\frac{1}{(2m\pi)^{2Q+2}}, \tag{E17}$$

which is bounded for all finite values of k. Now we have shown that the remainder $R_{\alpha,q}(k)$ is regular with no singularity in k, which completes the proof.

APPENDIX F: THE POSSIBLE SINGULARITY OF $\mathscr{F}_\alpha(k)$ OR $f_\alpha(k)$ FOR $\kappa_{l,\alpha}$ SATISFYING THE REGULARITY CONDITIONS

Corollary 1. If $\kappa_{l,\alpha}$ satisfies the regularity conditions (E1) and (E2), then $\mathscr{F}_\alpha(k)$ is regular as long as $k \neq 0$. The proof is straightforward: performing integration by part for the main integral in Eq. (E3), we find

$$\begin{aligned}\int_1^{N/2-1} \sin(kx)\kappa_{x,\alpha}dx &= -\frac{\cos(kx)}{k}\kappa_{x,\alpha}\bigg|_{x=1}^{x=N/2-1} + \frac{\sin(kx)}{k^2}\kappa_{x,\alpha}^{(1)}\bigg|_{x=1}^{x=N/2-1} \cdots \\ &\quad + \frac{(-1)^Q}{k^{2Q}}\int_1^{N/2-1}\cos(kx)\kappa_{x,\alpha}^{(2Q+1)}. \end{aligned} \tag{F1}$$

Since the integral is bounded according to Eq. (E2), we find

$$|\mathscr{F}_\alpha(k)| \leqslant \sum_{m=1}^{2Q}\frac{\mathcal{C}_{m-1}(\alpha)}{k^m}. \tag{F2}$$

Thus, $f_\alpha(k)$ or $\mathscr{F}_\alpha(k)$ are bounded as long as $k \neq 0$. From this proof, we immediately see that the only possible singularity of $\mathscr{F}_\alpha(k)$ is at $k = 0$. As we have mentioned in the main text, we can introduce a trick to get a rough estimate about the possible singularity of the main integral $\mathscr{F}_\alpha(k)$ near $k = 0$. We integrate over k from $1/N$ to Λ, where Λ is finite. This yields

$$\int_{1/N}^{\Lambda} dk\,\mathscr{F}_\alpha(k) = \int_1^{N/2-1}\frac{\kappa_{x,\alpha}}{x}dx - \int_1^{N/2-1}\frac{\kappa_{x,\alpha}\cos(\Lambda x)}{x}dx, \tag{F3}$$

where we have interchanged the order of integration. According to Appendix G, the second integral on the right-hand side of Eq. (F3) is bounded and the exact scaling with respect to N can be easily found by integrating by parts. Therefore, the scaling of $\int_{1/N}^{\Lambda}\mathscr{F}_\alpha(k)dk$ is totally controlled by the first integral on the right-hand side of Eq. (F3). If the scaling of $\int_{1/N}^{\Lambda}\mathscr{F}_\alpha(k)dk$ can be computed, it can reveal *some partial* information about the singularity of $\mathscr{F}_\alpha(k)$ around $k = 0$. For example, if $\int_{1/N}^{\Lambda}\mathscr{F}_\alpha(k)dk \sim$ constant or $\int_{1/N}^{\Lambda}\mathscr{F}_\alpha(k)dk \sim \ln N$, then we know the singularity of $\mathscr{F}_\alpha(k)$ at $k = 0$ is at most $1/k^{1-\varepsilon}$ or $1/k$, respectively, where ε is an arbitrary small positive number.

APPENDIX G: THE CONVERGENCE OF THE INTEGRAL $\int_1^\infty \kappa_{x,\alpha}\cos(\Lambda x)/x]dx$

One can prove the integral $\int \kappa_{x,\alpha}\cos(\Lambda x)/x]dx$ is bounded via integration by parts. First, it is found checked that

$$\begin{aligned}\int_1^\infty \kappa_{x,\alpha}\cos(\Lambda x)/x]dx &= \frac{1}{\Lambda}\sin(\Lambda x)\frac{\kappa_{x,\alpha}}{x}\bigg|_{x=1}^{x=\infty} \\ &\quad + \frac{1}{\Lambda}\int_1^\infty \sin(\Lambda x)\frac{\kappa_{x,\alpha}}{x^2} - \frac{1}{\Lambda}\int_1^\infty \sin(\Lambda x)\frac{\kappa_{x,\alpha}^{(1)}}{x}. \end{aligned} \tag{G1}$$

According to regularity condition (E1) of $\kappa_{x,\alpha}$, we know

$$\left|\int_1^\infty \sin(\Lambda x)\frac{\kappa_{x,\alpha}}{x^2}\right| \leqslant \mathcal{C}_{\max,\alpha}\left|\int_1^\infty \frac{1}{x^2}\right| < \infty, \tag{G2}$$

where

$$\mathcal{C}_{\max,\alpha} \equiv \max_{x\in[1,\infty]}\kappa_{x,\alpha}. \tag{G3}$$

The convergence of $\int_1^\infty \kappa_{x,\alpha}\cos(\Lambda x)/x]dx$ will depend on the convergence $\int_1^\infty \sin(\Lambda x)\kappa_{x,\alpha}^{(1)}/x$. Further integrating by parts and applying the same argument, one can show that the convergence of $\int_1^\infty \sin(\Lambda x)\kappa_{x,\alpha}^{(1)}/x$, will depend on $\int_1^\infty \cos(\Lambda x)\kappa_{x,\alpha}^{(2)}/x$. We continue to apply integration by parts until we obtain $\int_1^\infty \sin(\Lambda x)\kappa_{x,\alpha}^{(2Q+1)}/x$, which yields,

$$\begin{aligned}\int_1^\infty \kappa_{x,\alpha}\cos(\Lambda x)/x]dx &= \frac{1}{\Lambda}\sin(\Lambda x)\frac{\kappa_{x,\alpha}}{x}\bigg|_{x=1}^{x=\infty} + \frac{1}{\Lambda}\int_1^\infty \sin(\Lambda x)\frac{\kappa_{x,\alpha}}{x^2} \\ &\quad + \frac{1}{\Lambda^2}\cos(\Lambda x)\frac{\kappa_{x,\alpha}^{(1)}}{x}\bigg|_{x=1}^{x=\infty} + \frac{1}{\Lambda^2}\int_1^\infty \cos(\Lambda x)\frac{\kappa_{x,\alpha}^{(1)}}{x^2} \\ &\quad + \cdots + \frac{1}{\Lambda^{2Q+2}}\int_1^\infty \cos(\Lambda x)\frac{\kappa_{x,\alpha}^{(2Q+1)}}{x^2}. \end{aligned} \tag{G4}$$

Once again all the boundary terms in the above equations are bounded thanks to the regularity condition (E1). Furthermore, as with Eq. (G2), we note

$$\left|\int_1^\infty \sin(\Lambda x)\frac{\kappa_{x,\alpha}^{(2q)}}{x^2}\right| \leqslant \mathcal{C}_{\max,\alpha}^{(2q)}\left|\int_1^\infty \frac{1}{x^2}\right| < \infty, \tag{G5}$$

$$\left|\int_1^\infty \cos(\Lambda x)\frac{\kappa_{x,\alpha}^{(2q+1)}}{x^2}\right| \leqslant \mathcal{C}_{\max,\alpha}^{(2q+1)}\left|\int_1^\infty \frac{1}{x^2}\right| < \infty, \tag{G6}$$

where $q = 1, 2, \ldots, Q$ and

$$\mathcal{C}_{\max,\alpha}^{(q)} \equiv \max_{x\in[1,\infty]}\left|\kappa_{x,\alpha}^{(q)}\right|. \tag{G7}$$

Thus, the convergence of $\int_1^\infty \kappa_{x,\alpha}\cos(\Lambda x)/x]dx$ depends on $\int_1^\infty \sin(\Lambda x)\kappa_{x,\alpha}^{(2Q+1)}/x$. We use

$$\left|\int_1^\infty \cos(\Lambda x)\frac{\kappa_{x,\alpha}^{(2Q+1)}}{x^2}\right| \leqslant \left|\int_1^\infty \kappa_{x,\alpha}^{(2Q+1)}\right| < \infty \tag{G8}$$

according to the regularity condition (E2). We conclude that the integral $\int_1^\infty \kappa_{x,\alpha}\cos(\Lambda x)/x]dx$ is convergent.

According to Theorem 2, we find $f_\alpha(k) \sim \mathscr{F}_\alpha(k) \equiv \int_1^{N/2-1}\sin(kx)\kappa_{x,\alpha}dx$. Furthermore, according to Corollary 1, the only possible singularity of $\mathscr{F}_\alpha(k)$ is near $k = 0$. Using the trick in Eq. (F3), one can obtain some information about the behavior of $\mathscr{F}_\alpha(k)$ around $k = 0$ by investigating the scaling of $\int_{1/N}^{\Lambda}\mathscr{F}_\alpha(k)dk$ with Λ being any finite number. As we have shown above, the second term on the right-hand side of Eq. (F3) is convergent, and the scaling of $\int_{1/N}^{\Lambda}\mathscr{F}_\alpha(k)dk$ with respect to N is the same as the one of $\int_1^N \kappa_{x,\alpha}/x\,dx$. An immediate consequence is that the singularity of $\mathscr{F}_\alpha(k)$ is at most $O(1/k)$ since $\int_1^N(\kappa_{x,\alpha}/x)dx \leqslant \mathcal{C}_{\max,\alpha}\int_1^N 1/x\,dx \sim \ln N$, where $\mathcal{C}_{\max,\alpha} = \max_{x\in[1,\infty]}\kappa_{x,\alpha}$.

APPENDIX H: FINITE-SIZE SCALING

We note that Eq. (27) in the main text gives the asymptotic scaling of $I_0(\Delta)$ in the thermodynamics limit $N \to \infty$. For $\kappa_{x,\alpha} = x^{-\alpha}$, super-HS transition only occurs at $\alpha = 0$ for $N \to \infty$. However, for large but finite N, small α near zero may also lead the super-HS, which we now discuss. Setting $\alpha = \epsilon$, where ϵ is a small number, we obtain

$$\begin{aligned}\int_1^N \frac{dx}{x^{1+\epsilon}} &= \int_1^N dx \frac{1}{x} e^{-\ln x\epsilon} \\ &= \int_1^N dx \frac{1}{x}\left[\sum_{n=0}^{\infty} \frac{(-1)^n \epsilon^n (\ln x)^n}{n!}\right] \\ &= \sum_{n=0}^{\infty} \frac{(-1)^n \epsilon^n}{n!} \int_1^N dx \frac{(\ln x)^n}{x} = \mathcal{S}(\epsilon \ln N) \ln N,\end{aligned} \tag{H1}$$

where

$$\mathcal{S}(a) \equiv \sum_{n=0}^{\infty} \frac{(-1)^n a^n}{(n+1)!}. \tag{H2}$$

Therefore, we find when

$$\epsilon \ln N \ll 1, \tag{H3}$$

$\mathcal{S}(\epsilon \ln N) \to 1$ so that

$$\int_1^N \frac{dx}{x^{1+\epsilon}} \sim \ln N. \tag{H4}$$

Alternatively, $\mathcal{S}(a)$ may be evaluated exactly, which is

$$\mathcal{S}(a) = -\frac{1}{a} \sum_{n=1}^{\infty} \frac{(-1)^n a^n}{n!} = \frac{1}{a}(1 - e^{-a}). \tag{H5}$$

From which one can clearly see that $\mathcal{S}(\epsilon \ln N) \to 1$ as $\epsilon \ln N \to 0$. Therefore, according to Eq. (27) in the main text, we see that for $\kappa_{x,\epsilon} = x^{-\epsilon}$, we have

$$I_0(\Delta) \sim N^2 (\ln N)^2 \quad \text{for } \epsilon \ll (\ln N)^{-1}. \tag{H6}$$

By similar analysis, one can show analogously that for $\kappa_{x,\,1+\epsilon} = (1 + \ln x)^{-(1+\epsilon)}$

$$I_0(\Delta) \sim N^2 (\ln \ln N)^2 \quad \text{for } \epsilon \ll (\ln \ln N)^{-1}. \tag{H7}$$

APPENDIX I: THE LRK HAMILTONIAN IN THE SPIN REPRESENTATION

With the Jordan-Wigner transformation [34],

$$a_j^\dagger = (-1)^{j-1} \prod_{k=1}^{j-1} \sigma_k^z \sigma_j^+, \tag{I1}$$

$$a_j = (-1)^{j-1} \prod_{k=1}^{j-1} \sigma_k^z \sigma_j^-, \tag{I2}$$

where σ_j^z is the standard Pauli z matrix,

$$\sigma_j^+ \equiv \begin{bmatrix} 0 & 1 \\ 0 & 0 \end{bmatrix}, \tag{I3}$$

$$\sigma_j^- \equiv \begin{bmatrix} 0 & 0 \\ 1 & 0 \end{bmatrix}, \tag{I4}$$

it is readily checked that

$$a_j^\dagger a_j = \sigma_j^+ \sigma_j^- = \tfrac{1}{2}(\sigma_j^z + 1), \tag{I5}$$

$$a_{j+1}^\dagger a_j = -\sigma_{j+1}^+ \sigma_j^z \sigma_j^- = \sigma_{j+1}^+ \sigma_j^-, \tag{I6}$$

where we have used the fact $\sigma_j^z \sigma_j^\pm = \pm \sigma_j^\pm$ in the second equation. Furthermore,

$$\begin{aligned} a_j a_{j+l} &= (-1)^{j-1} \prod_{k=1}^{j-1} \sigma_k^z \sigma_j^- (-1)^{j+l-1} \prod_{m=1}^{j-1+l} \sigma_m^z \sigma_{j+l}^- \\ &= (-1)^l \sigma_j^- \sigma_j^z \prod_{k=j+1}^{j-1+l} \sigma_k^z \sigma_{j+l}^- \\ &= (-1)^l \sigma_j^- \prod_{k=j+1}^{j-1+l} \sigma_k^z \sigma_{j+l}^-, \end{aligned} \tag{I7}$$

where we have used the fact that $\sigma_j^\pm \sigma_j^z = \mp \sigma_j^\pm$. Now using the relation,

$$\sigma_j^+ \equiv \tfrac{1}{2}(\sigma_j^x + i\sigma_j^y), \tag{I8}$$

$$\sigma_j^- \equiv \tfrac{1}{2}(\sigma_j^x - i\sigma_j^y), \tag{I9}$$

where σ_j^x and σ_j^y are standard Pauli x and y matrices, respectively, we find

$$\begin{aligned} \sigma_j^+ \sigma_{j+l}^- + \sigma_j^- \sigma_{j+l}^+ &= \tfrac{1}{4}(\sigma_j^x + i\sigma_j^y)(\sigma_{j+l}^x - i\sigma_{j+l}^y) \\ &\quad + \tfrac{1}{4}(\sigma_j^x - i\sigma_j^y)(\sigma_{j+l}^x + i\sigma_{j+l}^y) \\ &= \tfrac{1}{2}(\sigma_j^x \sigma_{j+l}^x + \sigma_j^y \sigma_{j+l}^y), \end{aligned} \tag{I10}$$

$$\begin{aligned} \sigma_j^+ \sigma_{j+l}^+ + \sigma_j^- \sigma_{j+l}^- &= \tfrac{1}{4}(\sigma_j^x + i\sigma_j^y)(\sigma_{j+l}^x + i\sigma_{j+l}^y) \\ &\quad + \tfrac{1}{4}(\sigma_j^x - i\sigma_j^y)(\sigma_{j+l}^x - i\sigma_{j+l}^y) \\ &= \tfrac{1}{2}(\sigma_j^x \sigma_{j+l}^x - \sigma_j^y \sigma_{j+l}^y). \end{aligned} \tag{I11}$$

Using Eqs. (I1), (I2), and (I10), the tunneling and kinetic terms become

$$\begin{aligned} \sum_{j=1}^{N} (a_j^\dagger a_{j+1} + a_{j+1}^\dagger a_j) &= \sum_{j=1}^{N} (\sigma_j^- \sigma_{j+1}^+ + \sigma_j^+ \sigma_{j+1}^-) \\ &= \frac{1}{2} \sum_{j=1}^{N} (\sigma_j^x \sigma_{j+l}^x + \sigma_j^y \sigma_{j+l}^y), \end{aligned} \tag{I12}$$

and

$$\sum_{j=1}^{L} \left(a_j^\dagger a_j - \frac{1}{2} \right) = \frac{1}{2} \sum_{j=1}^{L} \sigma_j^z, \tag{I13}$$

respectively. For the long-range superconducting terms with the antiperiodic boundary condition, one can easily obtain the following alternative form:

$$\sum_{j=1}^{N-1} \sum_{l=1}^{N-j} \kappa_{l,\alpha} a_j a_{j+l} = \frac{1}{2} \sum_{j=1}^{N} \sum_{l=1}^{N-1} \kappa_{l,\alpha} a_j a_{j+l}, \tag{I14}$$

and a similar equation for the term $\sum_{j=1}^{N-1}\sum_{l=1}^{N-j}\kappa_{l,\alpha}a_{j+l}^{\dagger}a_j^{\dagger}$. On the other hand, with Eqs. (I1), (I2), and (I11), we find

$$\sum_{j=1}^{N}\sum_{l=1}^{N-1}\kappa_{l,\alpha}\left(a_j a_{j+l}+a_{j+l}^{\dagger}a_j^{\dagger}\right)=\frac{1}{2}\sum_{j=1}^{N}\sum_{l=1}^{N-1}(-1)^l\kappa_{l,\alpha}\left(\sigma_j^x\sigma_{j+l}^x-\sigma_j^y\sigma_{j+l}^y\right)\sigma_{j+1}^z\cdots\sigma_{j+l-1}^z. \tag{I15}$$

Substituting Eqs. (I12)–(I15) into Eq. (6) in the main text yields the LRK Hamiltonian in the spin representation, i.e., Eq. (35) in the main text.

[1] C. Helstrom, The minimum variance of estimates in quantum signal detection, IEEE Trans. Inf. Theory **14**, 234 (1968).
[2] C. W. Helstrom, *Quantum Detection and Estimation Theory* (Academic, Academic Press INC, New York, 1976).
[3] A. S. Holevo, *Probabilistic and Statistical Aspects of Quantum Theory* (Springer, Springer Science+Business Media, Heidelberg, 2011).
[4] S. L. Braunstein and C. M. Caves, Statistical Distance and the Geometry of Quantum States, Phys. Rev. Lett. **72**, 3439 (1994).
[5] H. T. Quan, Z. Song, X. F. Liu, P. Zanardi, and C. P. Sun, Decay of Loschmidt Echo Enhanced by Quantum Criticality, Phys. Rev. Lett. **96**, 140604 (2006).
[6] P. Zanardi, P. Giorda, and M. Cozzini, Information-Theoretic Differential Geometry of Quantum Phase Transitions, Phys. Rev. Lett. **99**, 100603 (2007).
[7] L. Campos Venuti and P. Zanardi, Quantum Critical Scaling of the Geometric Tensors, Phys. Rev. Lett. **99**, 095701 (2007).
[8] S.-J. Gu, Fidelity approach to quantum phase transitions, Int. J. Mod. Phys. B **24**, 4371 (2010).
[9] M. M. Rams, P. Sierant, O. Dutta, P. Horodecki, and J. Zakrzewski, At the Limits of Criticality-Based Quantum Metrology: Apparent Super-Heisenberg Scaling Revisited, Phys. Rev. X **8**, 021022 (2018).
[10] Y. Chu, S. Zhang, B. Yu, and J. Cai, Dynamic Framework for Criticality-Enhanced Quantum Sensing, Phys. Rev. Lett. **126**, 010502 (2021).
[11] L. Garbe, M. Bina, A. Keller, M. G. A. Paris, and S. Felicetti, Critical Quantum Metrology with a Finite-Component Quantum Phase Transition, Phys. Rev. Lett. **124**, 120504 (2020).
[12] U. Mishra and A. Bayat, Driving enhanced quantum sensing in partially accessible many-body systems, Phys. Rev. Lett. **127**, 080504 (2021).
[13] G. Tóth, Multipartite entanglement and high-precision metrology, Phys. Rev. A **85**, 022322 (2012).
[14] P. Hyllus, W. Laskowski, R. Krischek, C. Schwemmer, W. Wieczorek, H. Weinfurter, L. Pezzé, and A. Smerzi, Fisher information and multiparticle entanglement, Phys. Rev. A **85**, 022321 (2012).
[15] L. Pezzè, M. Gabbrielli, L. Lepori, and A. Smerzi, Multipartite Entanglement in Topological Quantum Phases, Phys. Rev. Lett. **119**, 250401 (2017).
[16] H. Yuan and C.-H. F. Fung, Optimal Feedback Scheme and Universal Time Scaling for Hamiltonian Parameter Estimation, Phys. Rev. Lett. **115**, 110401 (2015).
[17] S. Pang and A. N. Jordan, Optimal adaptive control for quantum metrology with time-dependent Hamiltonians, Nat. Commun. **8**, 14695 (2017).
[18] J. Yang, S. Pang, and A. N. Jordan, Quantum parameter estimation with the Landau-Zener transition, Phys. Rev. A **96**, 020301(R) (2017).
[19] V. Giovannetti, S. Lloyd, and L. Maccone, Quantum Metrology, Phys. Rev. Lett. **96**, 010401 (2006).
[20] M. Beau and A. del Campo, Nonlinear Quantum Metrology of Many-Body Open Systems, Phys. Rev. Lett. **119**, 010403 (2017).
[21] S. Boixo, S. T. Flammia, C. M. Caves, and JM. Geremia, Generalized Limits for Single-Parameter Quantum Estimation, Phys. Rev. Lett. **98**, 090401 (2007).
[22] S. M. Roy and S. L. Braunstein, Exponentially Enhanced Quantum Metrology, Phys. Rev. Lett. **100**, 220501 (2008).
[23] D. Vodola, L. Lepori, E. Ercolessi, A. V. Gorshkov, and G. Pupillo, Kitaev Chains with Long-Range Pairing, Phys. Rev. Lett. **113**, 156402 (2014).
[24] D. Vodola, L. Lepori, E. Ercolessi, and G. Pupillo, Long-range Ising and Kitaev models: Phases, correlations and edge modes, New J. Phys. **18**, 015001 (2015).
[25] O. Viyuela, D. Vodola, G. Pupillo, and M. A. Martin-Delgado, Topological massive Dirac edge modes and long-range superconducting Hamiltonians, Phys. Rev. B **94**, 125121 (2016).
[26] Note that unless the Hamiltonian is multiplicative, $|\psi_\theta\rangle$, in general, may be not the same as the true physical state $\mathcal{U}_\theta(T)|\psi_0\rangle$. However, $|\psi_\theta\rangle$ is able to give the same QFI as the true physical state, see Ref. [17] for further justifications.
[27] S. Pang and T. A. Brun, Quantum metrology for a general Hamiltonian parameter, Phys. Rev. A **90**, 022117 (2014).
[28] M. Cabedo-Olaya, J. G. Muga, and S. Martínez-Garaot, Shortcut-to-adiabaticity-like techniques for parameter estimation in quantum metrology, Entropy **22**, 1251 (2020).
[29] A. del Campo, Shortcuts to Adiabaticity by Counterdiabatic Driving, Phys. Rev. Lett. **111**, 100502 (2013).
[30] A. Y. Kitaev, Unpaired Majorana fermions in quantum wires, Phys.-Usp. **44**, 131 (2001).
[31] J. Alicea, New directions in the pursuit of Majorana fermions in solid state systems, Rep. Prog. Phys. **75**, 076501 (2012).
[32] Note that they represent $\kappa_{l,\alpha}=(\lambda l)^{-\alpha}$ with $\lambda>0$ and $\alpha\geqslant 0$ and $\kappa_{l,\alpha}=[\ln(\lambda l)]^{-\alpha}$ with $\lambda>1$ and $\alpha\geqslant 0$. Without loss of generality, we will set $\lambda=1$ in the former case and $\lambda=e$ in the latter case.
[33] F. W. J. Olver, *NIST Handbook of Mathematical Functions Paperback and CD-ROM*, 1st ed. (Cambridge University Press, Cambridge, UK, 2010).
[34] P. Coleman, *Introduction to Many-Body Physics*, 1st ed. (Cambridge University Press, Cambridge, UK, 2015).
[35] H. Qiao, Y. P. Kandel, S. Fallahi, G. C. Gardner, M. J. Manfra, X. Hu, and J. M. Nichol, Long-Distance

Superexchange between Semiconductor Quantum-Dot Electron Spins, Phys. Rev. Lett. **126**, 017701 (2021).

[36] P. Richerme, Z.-X. Gong, A. Lee, C. Senko, J. Smith, M. Foss-Feig, S. Michalakis, A. V. Gorshkov, and C. Monroe, Non-local propagation of correlations in quantum systems with long-range interactions, Nature (London) **511**, 198 (2014).

[37] P. Jurcevic, B. P. Lanyon, P. Hauke, C. Hempel, P. Zoller, R. Blatt, and C. F. Roos, Quasiparticle engineering and entanglement propagation in a quantum many-body system, Nature (London) **511**, 202 (2014).

[38] C.-L. Hung, A. González-Tudela, J. I. Cirac, and H. J. Kimble, Quantum spin dynamics with pairwise-tunable, long-range interactions, Proc. Natl. Acad. Sci. USA **113**, E4946 (2016).

[39] H. Shapourian and S. Ryu, Entanglement negativity of fermions: Monotonicity, separability criterion, and classification of few-mode states, Phys. Rev. A **99**, 022310 (2019).

[40] J. Yang, S. Pang, Y. Zhou, and A. N. Jordan, Optimal measurements for quantum multiparameter estimation with general states, Phys. Rev. A **100**, 032104 (2019).

[41] S. Zhou, C.-L. Zou, and L. Jiang, Saturating the quantum Cramér–Rao bound using LOCC, Quantum Sci. Technol. **5**, 025005 (2020).

[42] K. Knopp, *Theory and Application of Infinite Series*, illustrated ed. (Dover, New York, 1990).

[43] C. M. Bender and S. A. Orszag, *Advanced Mathematical Methods for Scientists and Engineers I: Asymptotic Methods and Perturbation Theory* (Springer, New York, 2013).